UNIVERSITY OF CALIFORNIA,
IRVINE

Coherent Control of Diamond NV Centers with Chirped Laser Pulses

THESIS

submitted in partial satisfaction of the requirements
for the degree of

MASTER OF SCIENCE

in Electrical Engineering

by

Neilalohith Sharma

Thesis Committee:
Assistant Professor Maxim R. Shcherbakov, Chair
Professor Filippo Capolino
Professor Peter Burke

2023

TABLE OF CONTENTS

LIST OF FIGURES

ACKNOWLEDGEMENTS

I would like to express my deepest gratitude to Professor Maxim R. Shcherbakov for his generous support and funding throughout the completion of my master's thesis. His belief in my abilities and commitment to my academic and research endeavors have been instrumental in the successful completion of this work. His expertise, guidance, and insights have significantly shaped my research and have contributed immensely to my thesis.

I would also like to thank my committee members, Professor Filippo Capolino, and Professor Peter Burke, who provided valuable advice and comments on my work which led to better understanding the task at hand and led me to ask better questions. I am grateful for their encouragement and mentorship.

ABSTRACT OF THE THESIS

Coherent Control of Diamond NV Centers with Chirped Laser Pulses

by

Neilalohith Sharma

Master of Science in Electrical Engineering

University of California, Irvine, 2023

Assistant Professor Maxim R. Shcherbakov, Chair

This thesis explores the coherent control of diamond NV (nitrogen-vacancy) centers using chirped laser pulses. Diamond NV centers possess unique optical properties, making them promising candidates for quantum information processing and sensing. Chirped laser pulses offer a versatile approach to achieve efficient and robust control over NV center two-level systems.

The thesis begins with a theoretical analysis of the optical dynamics of NV centers interacting with an electromagnetic field. It establishes the Maxwell-Bloch equations and provides a set of differential equations that can be solved numerically via computer simulations.

The effects of varying electric field intensity and detuning in a continuous wave case are simulated. Later, the interaction between the NV center and a gaussian pulse is calculated. The pulse is then chirped both linearly and quadratically and the different modes of control that can be achieved are shown along with the optimal case for the linear and quadratic chirp.

Overall, this thesis establishes a foundation for exploring coherent control techniques with chirped laser pulses in diamond NV center systems that can also be applied to other two-level systems by changing the computational parameters. The results highlight the potential of chirped laser pulses for coherent control and provide insights for future experiments.

INTRODUCTION

Quantum systems consisting of two-level systems, such as spin qubits or atomic systems, have attracted significant interest in recent years due to their potential applications in quantum information processing and sensing. Coherent control techniques have been developed to manipulate the quantum state of these systems and enable precise control of their evolution. In this thesis, we explore coherent control techniques, through laser pulses, to manipulate the quantum state of two-level systems and improve their performance as quantum sensors or information processors. The two-level system being studied is the nitrogen vacancy (NV) center in diamond.

We begin by reviewing the basic principles of two-level systems, dynamics of Rabi oscillations, and the diamond NV center. Fundamental concepts of coherent control, through methods like varying electric field intensity, detuning, and chirped pulses.

Then, we focus on the use of coherent control techniques to enhance the sensitivity and precision of two-level systems as quantum sensors. We discuss optimization using linearly and quadratically chirped pulses.

Finally, we highlight some of the remaining challenges and opportunities in the field of coherent control of two-level systems.

Overall, this thesis provides an overview of the current state of the art in the field of coherent control of two-level systems and offers insights into the potential future directions for this rapidly evolving field.

1. Overview

i. Overview of Two-Level Systems

A two-level quantum system is a quantum mechanical system that has two basis states. These states are typically represented as basis vectors in a two-dimensional Hilbert space, often denoted as $|0\rangle$ and $|1\rangle$, which correspond to the ground state and excited state of the system, respectively.

In quantum mechanics, a two-level quantum system can be realized in various physical systems, such as a spin-half particle (e.g., an electron), a superconducting qubit, or a single photon. These systems are important in the context of quantum computing and quantum information processing, as a two-level system is essentially a qubit.

Rabi oscillations refer to the periodic and coherent oscillations between two energy states in a two-level quantum system. There are two energy eigenstates, typically referred to as the ground state (lower energy level) and the excited state (higher energy level). Rabi oscillations occur when the system is subjected to an external oscillating electromagnetic field, such as a laser pulse.

The application of the resonant field causes the probability amplitude of the ground state to decrease, while the probability amplitude of the excited state increases. As time progresses, these probability amplitudes undergo periodic oscillations. The oscillation frequency is known as the Rabi frequency.

Rabi sidebands refer to the spectral components that appear around the central frequency in the frequency spectrum of a system undergoing Rabi oscillations. The distance between these sidebands is of importance to us as it is directly related to the

rabi frequency. The appearance of Rabi sidebands can be understood from a Fourier analysis perspective. The periodic oscillations of the system due to Rabi oscillations can be decomposed into a series of harmonic components, each corresponding to a specific frequency. The presence of the sidebands indicates the existence of these harmonic components in the frequency spectrum.

In the following simulations, the quantity that is carefully studied is the transition dipole moment and its dynamics under laser stimulation. The transition dipole moment is a fundamental concept in quantum mechanics that describes the strength and direction of the interaction between two quantum states during a transition. It quantifies the likelihood of a transition occurring between two energy levels in a quantum system.

In quantum mechanics, transitions between energy levels are driven by the absorption or emission of electromagnetic radiation. The transition dipole moment characterizes the coupling strength between the initial and final states involved in the transition. It is represented by a vector quantity with both magnitude and direction.

Coherent control in two-level systems refers to the ability to manipulate the quantum state of a two-level system by applying precisely timed and tuned electromagnetic fields. By carefully controlling the frequency, amplitude, and phase of the electromagnetic field, it is possible to manipulate the interference between the two energy levels of the system, and to create well-defined superpositions of the two states.

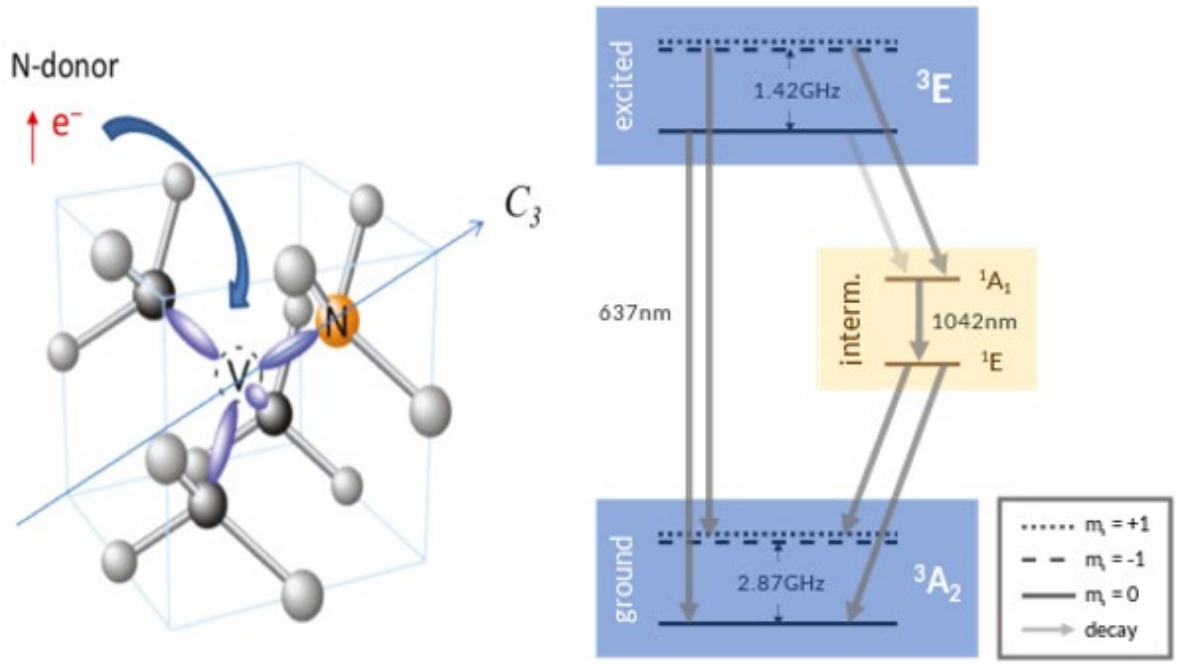

Figure 1: Diamond NV center on the left [2]. Band structure on the right. [https://commons.wikimedia.org/wiki/File:NV-energy-levels.svg, Wikimedia Commons]. We are concerned with the 637 nm transition.

The NV center is a defect in diamond that consists of a substitutional nitrogen atom and a vacancy located adjacent to each other. The NV center has unique optical and spin properties that make it attractive for various applications, including quantum sensing, magnetometry, and quantum information processing.

This thesis deals specifically with the optical transition in the NV center from the $^3A_2$ to the ^3E levels, which appears at 637 nm / 1.945 eV [2]. This corresponds to a transition frequency of 470.297 THz. Through ab initio calculations, it is found that this transition has a transition dipole moment of 5.2 Debye [2]. The relaxation time for this system is found to be 13 ns [3].

ii. **Review of Current Research**

Current research on coherent control explores techniques like resonant excitation: (applying a resonant electromagnetic field to the quantum system to induce transitions), adiabatic following (involves slowly varying the parameters of the system's Hamiltonian to ensure that the system remains in its ground state), and single-shot shaped pulses (involves designing a single pulse that is optimized for the specific task such as inducing a particular transition between energy levels) [5].

The effectiveness of detuned and chirped pulses in achieving robust transfer of a ground state to a desired coherent superposition with arbitrary amplitude and phase. has been demonstrated through numerical simulations and experimentally with ultrafast optical control of cold rubidium atoms. The proposed robust control method is achieved by temporal linear chirping and a static detuning applied to a Gaussian-shaped pulse [6].

Another concept called “adiabatic passage” is introduced. In the context of coherent control, adiabatic passage refers to a technique used to transfer a quantum system from one state to another without any significant population loss or excitation to other unwanted states. It is a process that relies on the slow and continuous variation of the system's parameters, such as the control fields or the energy levels, ensuring that the system remains in its instantaneous eigenstate throughout its evolution [5].

The idea is to match the initial state vector to one of the two instantaneous eigenvectors of the Hamiltonian and then guide the state vector in its Hilbert space to produce any desired superposition state. By adjusting the Hamiltonian time variation to be

appropriately slow (adiabatic), an experimenter can produce population alteration without requiring precise control of the pulse area and detuning.

Chirped pulses can have a significant impact on adiabatic passage by modifying the dynamics of the system during the population transfer process. Chirping refers to the intentional variation of the pulse frequency or phase over time, which can be linear, quadratic, or of a different functional form.

The effect of chirped pulses on adiabatic passage depends on the specific chirping scheme employed and its interaction with the system's energy levels and dynamics. Here are a few ways in which chirped pulses can affect adiabatic passage:

- Adiabaticity enhancement: Chirping the pulse can enhance the adiabaticity of the process. By carefully designing the chirping profile, the pulse frequency can be adjusted to match the changing energy levels of the system during the adiabatic passage. This ensures a better match between the system's eigenstates and the pulse, leading to improved population transfer efficiency [9].

- Increased robustness: Chirped pulses can enhance the robustness of adiabatic passage against certain experimental imperfections or variations in the system parameters. The chirping can help mitigate the effects of external noise, fluctuations, or imperfections in the control fields. It provides a certain level of tolerance to deviations from perfect adiabatic conditions, allowing for more reliable and efficient population transfer [9].

- Control of passage dynamics: The specific chirping scheme can be used to control the dynamics of the population transfer process. By carefully adjusting the chirp

rate and profile, one can manipulate the speed and shape of the adiabatic passage. This enables tailoring the transfer time, population transfer efficiency, and other characteristics of the process to match the desired experimental requirements.

On the other hand, non-adiabatic passage involves a rapid and abrupt transition between states, typically occurring when the evolution of the system is faster than the characteristic timescale associated with the energy gaps between states. In non-adiabatic processes, the system does not have enough time to adjust to the changing conditions, resulting in a non-adiabatic coupling between states. This can lead to population loss, excitations to other states, and the formation of unwanted interference patterns.

The use of ultra-chirped pulses to explore the limit of non-adiabatic passage have been explored. An “ultra-chirped pulse” is where the instantaneous frequency change is of the order of the transition frequency of the two-level system [7].

A fast and robust method of population transfer between two quantum states has been demonstrated with a quadratically chirped laser source. Transition probabilities have been obtained numerically and the conditions of the adiabatic passage have been explored [8].

The thesis explores adiabatic passage by means of chirping the gaussian pulse both linearly and quadratically. These chirps are optimized for two different cases: initially to bring the system to a relaxed state faster than an unchirped pulse and then to change the population transfer dynamics to ensure the transfer is confined and enhanced in the pulse area.

2. Model

i. Optical Stark Effect

The optical Stark effect (OSE), (sometimes called the AC Stark effect or Autler–Townes effect), refers to the phenomenon in which the energy levels of a quantum system are modified by the presence of an external alternating electric field. When an external alternating electric field is applied, it interacts with the charge distribution of the system, leading to a Stark shift in the energy levels. The magnitude of the Stark shift depends on the electric field intensity, the resonant frequency of the system, and the frequency of the driving field, among other things. In the case of the optical Stark effect, the external field is usually provided by a laser beam.

The model used to describe the OSE is typically based on a two-level system interacting with an external electromagnetic field, such as a laser field. The interaction is governed by the Hamiltonian of the system, which includes terms representing the energy levels, the electric dipole moment, and the interaction with the electromagnetic field. The basic model can be described by the Hamiltonian:

$$\hat{H} = \hat{H}_0 + \hat{V}(t), \tag{1}$$

where $\hat{H}_0$ represents the unperturbed Hamiltonian of the two-level system, and $\hat{V}(t)$ represents the perturbation due to the interaction with the laser field. The unperturbed Hamiltonian $\hat{H}_0$ typically includes terms representing the energy levels and their associated energies, such as the ground state and the excited state of the system. The energies of the energy levels are often denoted as E_a and E_b, respectively and the transition takes place from a to b with a transition frequency ω_{ba} [1].

The perturbation term $\hat{V}(t)$ accounts for the interaction between the two-level system and the laser field. It is typically described using the dipole approximation, which assumes that the system's interaction with the electromagnetic field is primarily due to the electric dipole moment associated with the energy level transitions. The dipole moment is represented by the operator $\hat{\mu}$.

The interaction term $\hat{V}(t)$ can be written as:

$$\hat{V}(t) = -\hat{\mu}\tilde{E}(t), \tag{2}$$

where $\tilde{E}(t)$ represents the electric field of the laser at time t. Elements of the system are described explicitly with a density matrix.

$$\hat{\rho} = \begin{bmatrix} \rho_{aa} & \rho_{ab} \\ \rho_{ba} & \rho_{bb} \end{bmatrix}. \tag{3}$$

Just as the Schrödinger equation describes how pure states evolve in time, the von Neumann equation describes how a density operator evolves in time. The evolution of the density matrix without damping can be written as:

$$\dot{\rho}_{nm} = -\frac{i}{\hbar}\left[\hat{H}, \hat{\rho}\right]_{nm}$$

$$= -\frac{i}{\hbar}\left[\left(\hat{H}\hat{p}\right)_{nm} - \left(\hat{p}\hat{H}\right)_{nm}\right]$$

$$= -\frac{i}{\hbar}\sum_v (H_{nv}\rho_{vm} - \rho_{nv}H_{vm}). \tag{4}$$

We now introduce the decomposition of the Hamiltonian into atomic and interaction parts into this expression to obtain:

$$\dot{\rho}_{nm} = -i\omega_{nm}\rho_{nm} - \frac{i}{\hbar}\sum_v (V_{nv}\rho_{vm} - \rho_{nv}V_{vm}), \tag{5}$$

where $n,\ m,$ and v take values of a or b from the density matrix, $\omega_{nm} = \frac{E_n - E_m}{\hbar}$ is the transition frequency, V is the interacting term in the dipole. ρ_{aa} and ρ_{bb} represent the probabilities of occupation and add up to 1 and their derivatives in time add to 0 (conserved) [1].

By solving the above for a two-level atom with relaxation times T_1 and T_2, where T_1 is called the population relaxation time and T_2 is the dephasing time, one can obtain the time evolution of the system's wavefunction and calculate the energy level shifts caused by the interaction with the laser field. This allows for the prediction and understanding of the observed spectral changes and shifts in the optical absorption or emission spectrum due to the optical Stark effect.

The time evolution of the density matrix elements with relaxation times is:

$$\frac{d\rho_{ba}}{dt} = -\left(i\omega_{ba} + \frac{1}{T_2}\right)\rho_{ba} + \frac{i}{\hbar}V_{ba}(\rho_{bb} - \rho_{aa}), \tag{6.1}$$

$$\frac{d(\rho_{bb}-\rho_{aa})}{dt} = -\frac{(\rho_{bb}-\rho_{aa})-(\rho_{bb}-\rho_{aa})^{(eq)}}{T_1} - \frac{2i}{\hbar}(V_{ba}\rho_{ab} - \rho_{ba}V_{ab}). \tag{6.2}$$

ii. Maxwell-Bloch Equations

The optical Bloch equations/Maxwell-Bloch equations describe the dynamics of a two-level quantum system interacting with an external electromagnetic field, such as a laser field. These equations provide a mathematical framework to analyze the time evolution of the system's coherence and populations under the influence of the field.

The rotating wave approximation (RWA) is used when the frequency detuning between the field and the atomic transition is much smaller than the characteristic frequencies of the system.

The optical Bloch equations under the RWA is a simplified model that neglects certain terms in the interaction Hamiltonian to simplify the calculations. The RWA assumes that the frequency of the laser field is close to resonance with a particular energy level transition [1].

The interaction term between the two-level system and the laser field is expressed as:

$$\hat{V}(t) = -\hat{\mu}\tilde{E}(t)e^{i\omega t} + \text{h.c.} \tag{7}$$

where μ is the electric dipole moment operator, $E(t)$ is the electric field of the laser, ω is the angular frequency of the laser field, and h.c. denotes the Hermitian conjugate.

The key approximation made under the RWA is to neglect the rapidly oscillating term $e^{i\omega t}$ with respect to the other terms in the interaction Hamiltonian. This approximation is valid when the detuning between the laser frequency and the energy level transition frequency is much smaller than the energy level splitting. By neglecting the rapidly oscillating terms, the interaction Hamiltonian simplifies to:

$$\hat{V}(t) \approx -\hat{\mu}\tilde{E}(t) + \text{h.c.} \tag{8}$$

With the RWA, the time-dependent von Neumann equation can be solved to obtain the time evolution of the system's wavefunction and calculate the energy level shifts induced by the laser field. The RWA simplifies the calculations by removing the fast-oscillating terms, making the problem more easily modelled computationally.

Under the RWA, V_{ba} term can be replaced with $-\mu_{ba}Ee^{-i\omega t}$, assuming the system is being driven at an ω different to the transition frequency [1].

Another term, a slowly varying quantity σ_{ba} is introduced: $\rho_{ba}(t) = \sigma_{ba}(t)e^{-i\omega t}$. To form the Maxwell-Bloch equations, a complex amplitude of the dipole moment p, population inversion w and a coupling constant κ is introduced:

$p = \sigma_{ba}\mu_{ab}$,

$w = \rho_{bb} - \rho_{aa}$,

$\kappa = \frac{2\mu_{ba}}{\hbar}$.

Making the above substitutions made in the equations for the time evolution of the density matrix (Es**.** 6.1 and 6.2) we get the optical Bloch equations for a two-level system under a constant field, written as:

$$\frac{dp}{dt} = \left(i\Delta - \frac{1}{T_2}\right)p - \frac{\hbar}{4}i|\kappa|^2 Ew \tag{9.1}$$

$$\frac{dw}{dt} = -\frac{w-w^{(eq)}}{T_1} - \frac{4}{\hbar}\mathrm{Im}(Ep^*) \tag{9.2}$$

Where:

- p is the transition dipole moment associated with the system. It is a complex number. The SI unit of dipole moment is C.m and all figures are expressed in it. Dipole moment is expressed as a real number obtained from $pe^{-i\omega_o t} + \mathrm{c.c.}$ where ω_o is the transition frequency.

- Δ is the detuning i.e., the difference between the driving frequency (ω) and the transition frequency (ω_{ba})
- E is the electric field strength in V/m.
- w is the population inversion. It is a fraction that ranges from -1 (population entirely in ground state) to +1 (entirely in excited state). $w^{(eq)}$ is assumed to be 0, at equilibrium.
- $\hbar$ is Reduced Planck's constant.
- κ is a coupling constant. $\kappa = \frac{2\mu_{ba}}{\hbar}$. μ_{ba} is the transition dipole moment and is approximately 5.2 Debye for this transition in the diamond NV center.
- T_1 is called the population relaxation time and T_2 is the dephasing time. T_2 for this system is 13 ns at 273K. T_1 is of the order of T_2 and can be approximated to $\frac{T_2}{2}$

3. Results

i. Continuous wave excitation:

When a two-level system interacts with an oscillating external field, it produces Rabi oscillations.

Here, the Rabi oscillations refer to the periodic and coherent oscillations between two quantum states induced by the interaction with an external electromagnetic field (laser).

The basic principle behind Rabi oscillations is as follows: When a two-level quantum system is subjected to a resonant optical field, the energy levels of the system are split, forming a coherent superposition of the two states. This superposition evolves in time, leading to oscillations between the two states.

Initially, if the system is in the ground state, application of the resonant optical field will cause it to start oscillating between it and the excited state.

The resonant field causes the probability amplitude of the ground state to decrease, while the probability amplitude of the excited state increases. As time progresses, these probability amplitudes undergo periodic oscillations.

The amplitude of the oscillation depends on the strength of the applied field, characterized by the Rabi frequency (Ω_o). The Rabi frequency is determined by the intensity of the field and the dipole moment associated with the transition between the two states.

The dynamics of Rabi oscillations can be described mathematically the optical Bloch equations as mentioned previously.

With reference to these, the Rabi frequency $\Omega_o = \frac{\mu_{ba}E}{\hbar}$, where E is the electric field strength and μ_{ba} is the transition dipole moment [1].

For a case where there is a finite detuning, the rabi frequency is expressed an equivalent Rabi frequency $\Omega = \sqrt{\Omega_o^2 + \Delta^2}$ where Δ is the detuning (the difference between the driving frequency ω and the transition frequency ω_{ba}).

Rabi sidebands are spectral features that arise in the optical spectrum of a two-level quantum system undergoing Rabi oscillations. The interaction with the laser field causes the splitting of the spectral line associated with the transition between the two states.

The Rabi sidebands appear as two symmetric peaks around the central transition frequency in the system's optical spectrum. The separation between the sidebands is equal to twice the equivalent Rabi frequency (2Ω).

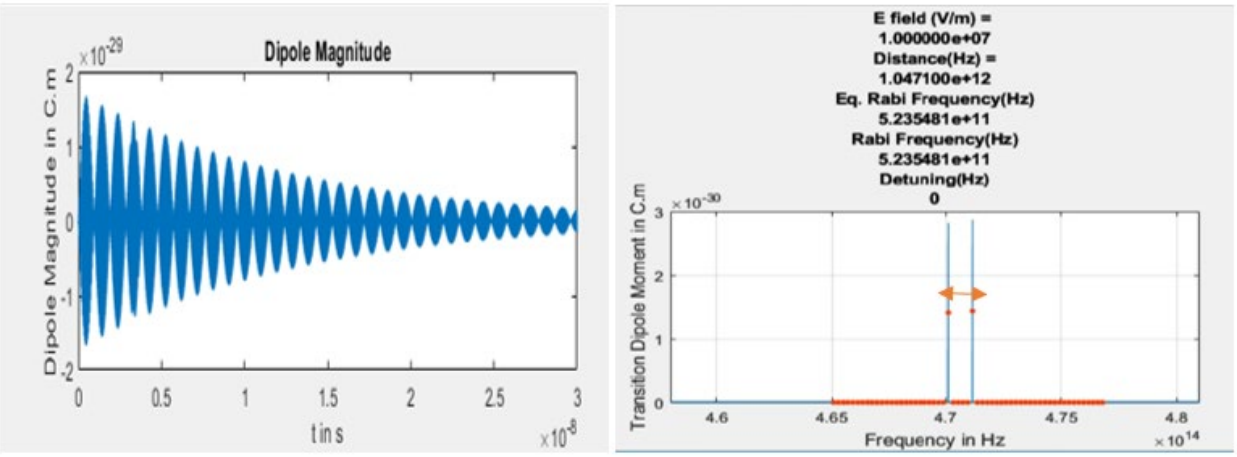

Figure 2: Temporal plot of Rabi oscillations at 10^7 V/m field strength on the right. Fourier transform on the left showing the Rabi sidebands.

The above figure shows Rabi oscillations in this system at an electric field strength of 10^7 V/m and driving frequency equal to the fundamental frequency i.e., no detuning. The distance between the two sidebands can be seen in the Fourier transform on the right. The sidebands are centered around the fundamental frequency and the distance between is exactly twice the Rabi frequency.

Thus, two methods arise for controlling this two-level system.

a. Varying Electric Field Strength (CW)

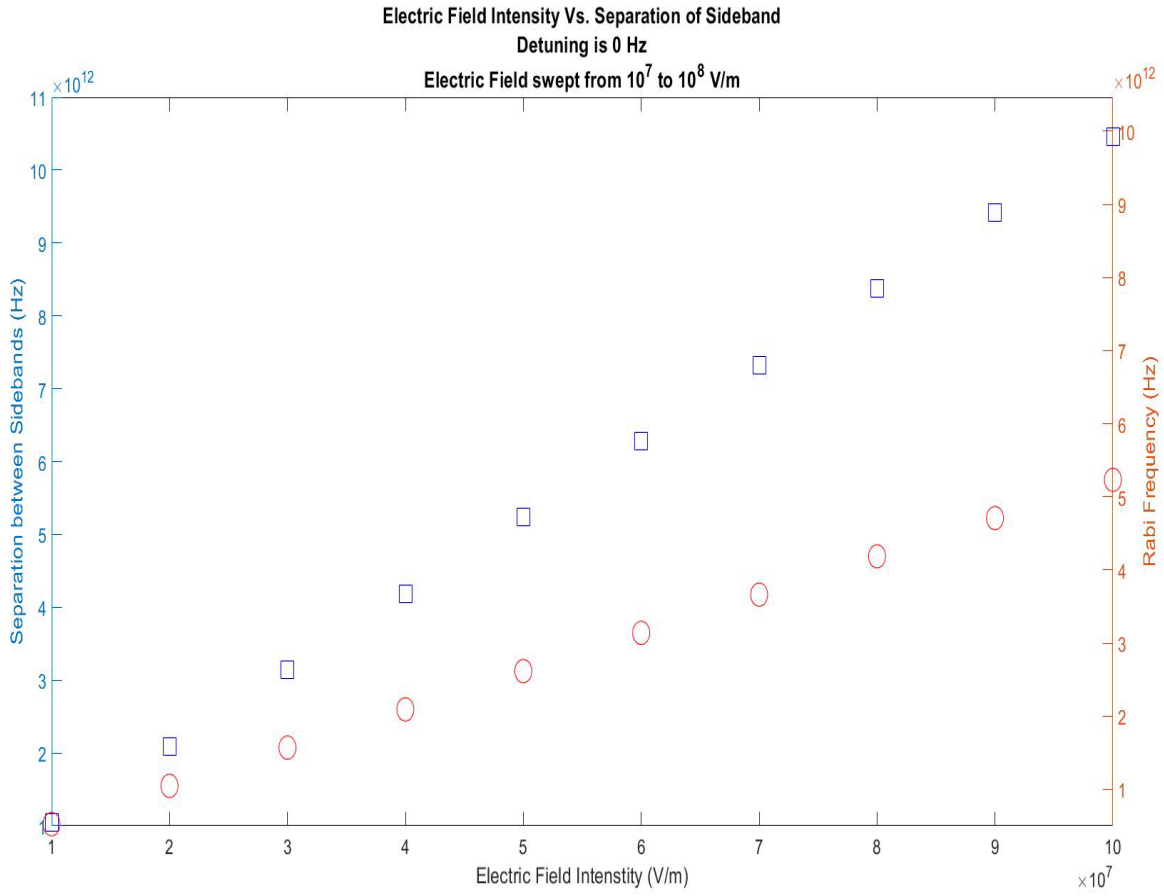

Figure 3 Separation between the sidebands as electric field intensity is swept. It is linear and twice the Rabi frequency. Detuning is 0 Hz

The figure shows the separation between the sidebands as a linear function of electric field intensity. Also plotted is the Rabi frequency as a function of the same.

b. Varying the Detuning

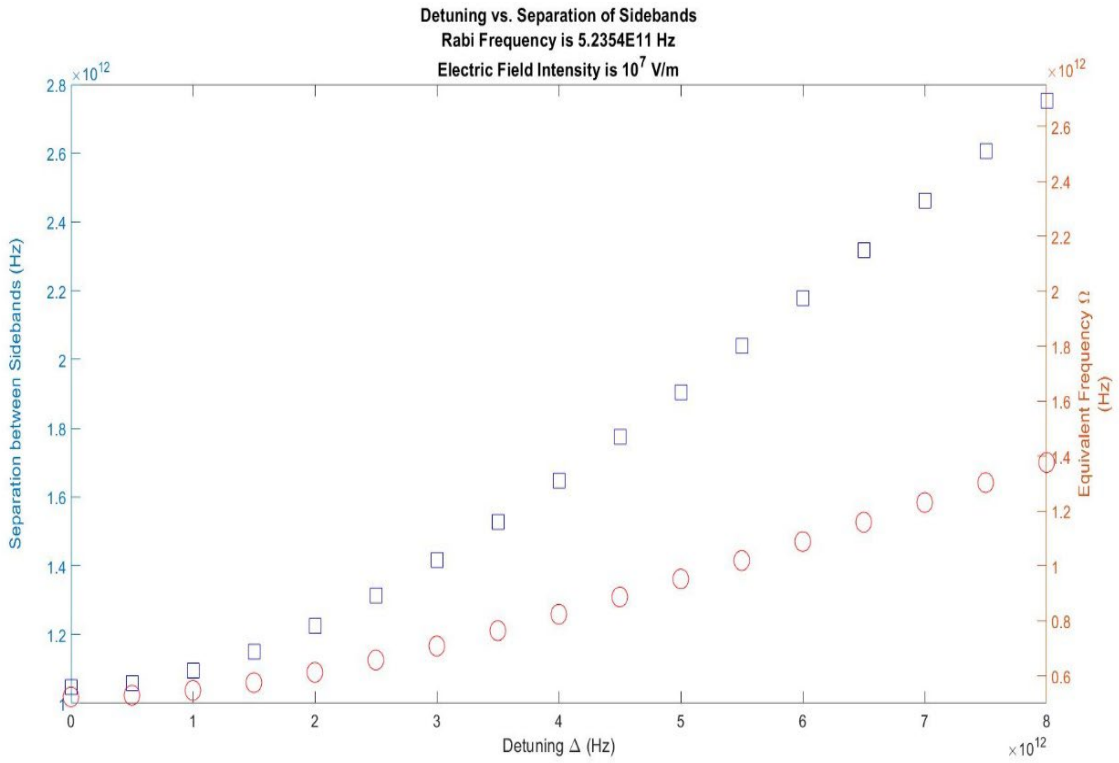

Figure 4: Separation between sidebands as a function of detuning, at constant electric field. Nonlinear relationship when detuning is small compared to the Rabi frequency but becomes linear as it the detuning increases.

The above figure shows the separation between the sidebands as a function of detuning (Δ). The separation between the sidebands is double the equivalent Rabi frequency ($\sqrt{\Delta^2 + \Omega_0^2}$), at constant electric field (10^7 V/m).

At low detuning, when it is much less than the rabi frequency, the separation is not linear.

As the detuning increases to where $\Delta \gg \Omega_o$, then the separation becomes linear.

ii. Unchirped Gaussian Pulse

For practical considerations, to achieve high electric field intensities, pulsed laser operation is necessary. Picosecond and femtosecond laser pulses can be used. Mathematically, it is expressed as $E = E_0 e^{-i\omega t} e^{-\frac{(t-t_0)^2}{(2\tau)^2}}$ where τ is the width of the pulse and t_0 is the center of the pulse.

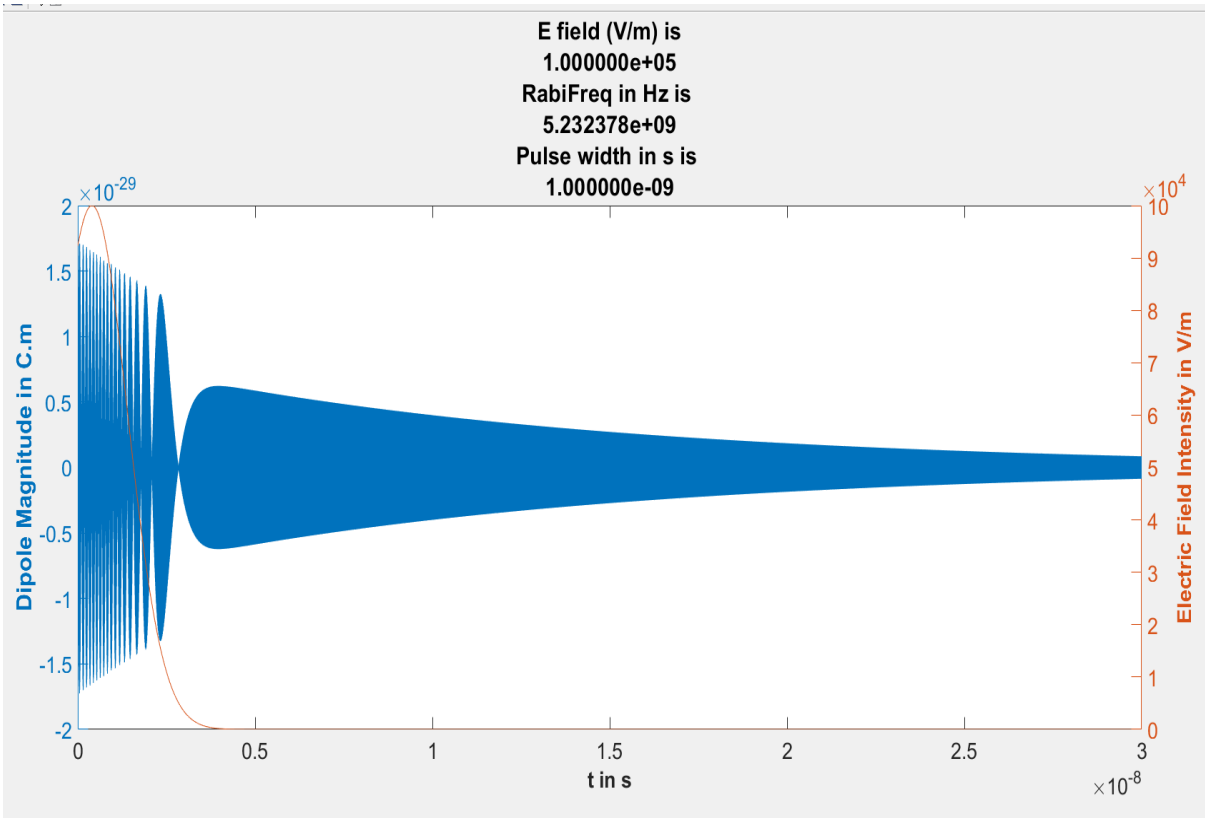

Figure 5: Rabi oscillations under a Gaussian pulse.

The above picture illustrates the behavior of the Rabi oscillations under a Gaussian pulse. The oscillations are more frequent in the region of the pulse where it has the most energy and slows down as the energy decreases till at a point the system starts to relax.

iii. Chirped Pulses:

The figure below shows a spectrogram of the various chirps that are applied to the gaussian pulse to gain more control over the system.

They are all gaussian pulses centered at 1 ns and have a width of 100 ps. The maximum intensity is confined around the peak of the pulse, at 1 ns. The following simulations calculate the behavior of the TLS stimulated by a chirped Gaussian pulse.

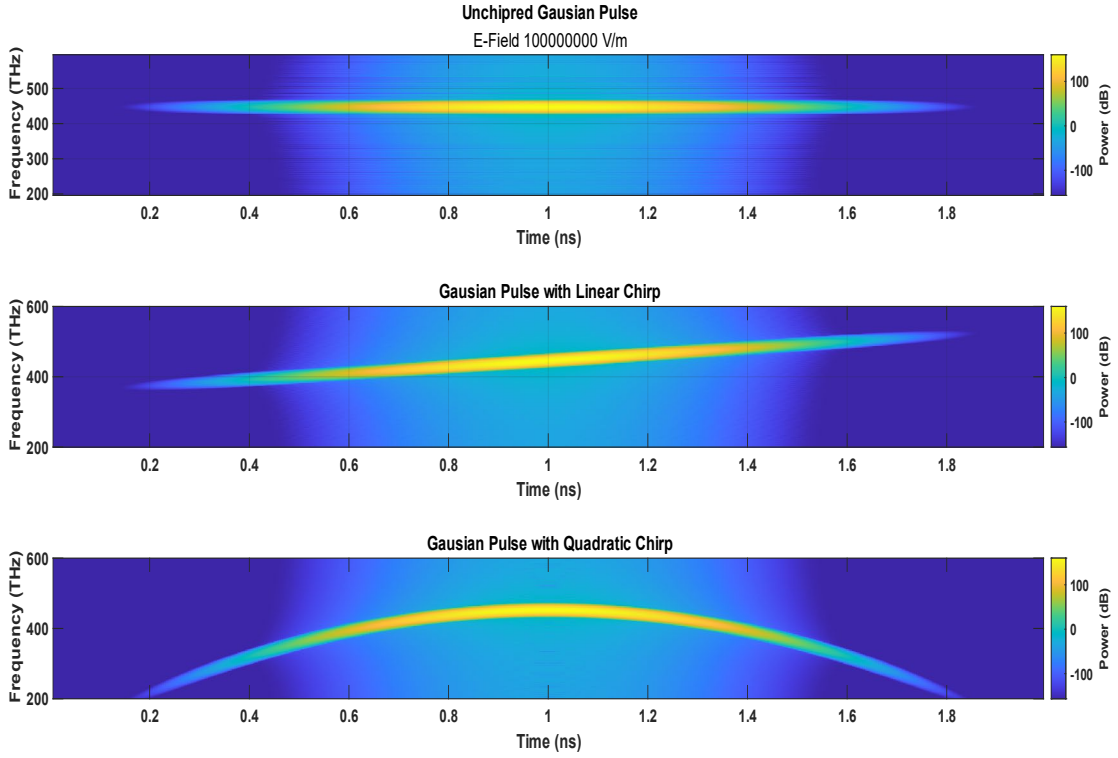

Figure 6: Spectrogram of unchirped, linearly chirped, and nonlinear (quadratic) chirped Gaussian pulses that are centered at 1 ns and are 100 ps wide.

a. Control with Linear Chirp

The figure shows the type of chirp that is applied to that gaussian pulse. The linear chirp has a chirp factor of α (Hz) that is described by the equation:

$$E = E_0 e^{-i\omega(1+\alpha t/2)t} e^{-\frac{(t-t_0)^2}{(2\tau)^2}}.$$

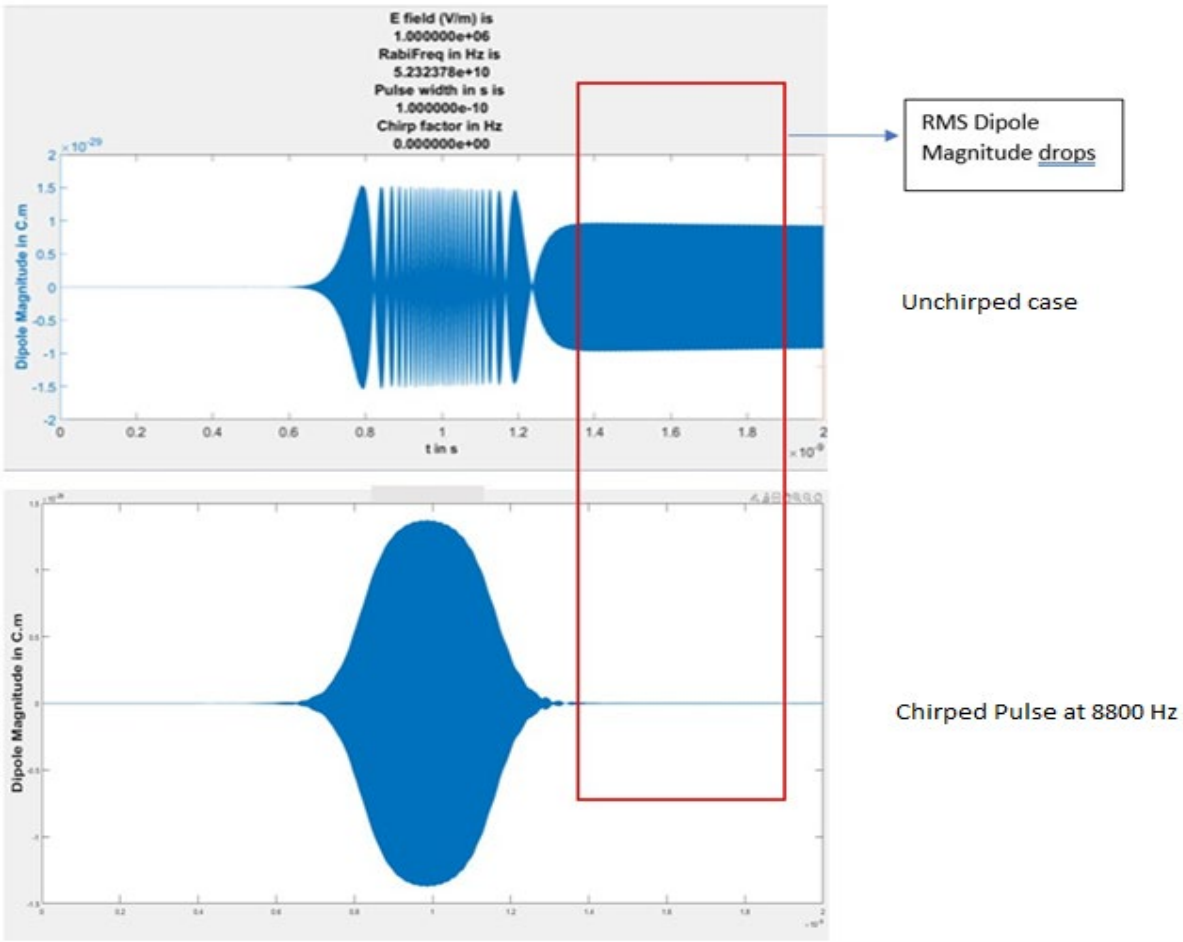

Figure 7: The RMS value of the region in the red box is calculated. This is for a small period right after the duration of the pulse. It measures if the system has relaxed.

From the above, at a particular linear chirp, the dipole moment (calculated as a root mean square) of system drops a few orders of magnitude from its peak much quicker than in the case without any chirp. The system is forced to relax faster than its slow dephasing time would normally allow.

The figure below shows a sweep of the chirp from 10 Hz (nearly unchirped) to 10,000 Hz. The dipole magnitude after duration of the pulse is calculated and we see there is a roll off after which it reaches a minimum after a particular frequency.

This is repeated with increasing electric field intensities. Another observation is that with increasing intensities, the chirp at which the dipole moment is minimum (chirp for forcing the system to relax) also increases as indicated with the black lines marked on the x-axis.

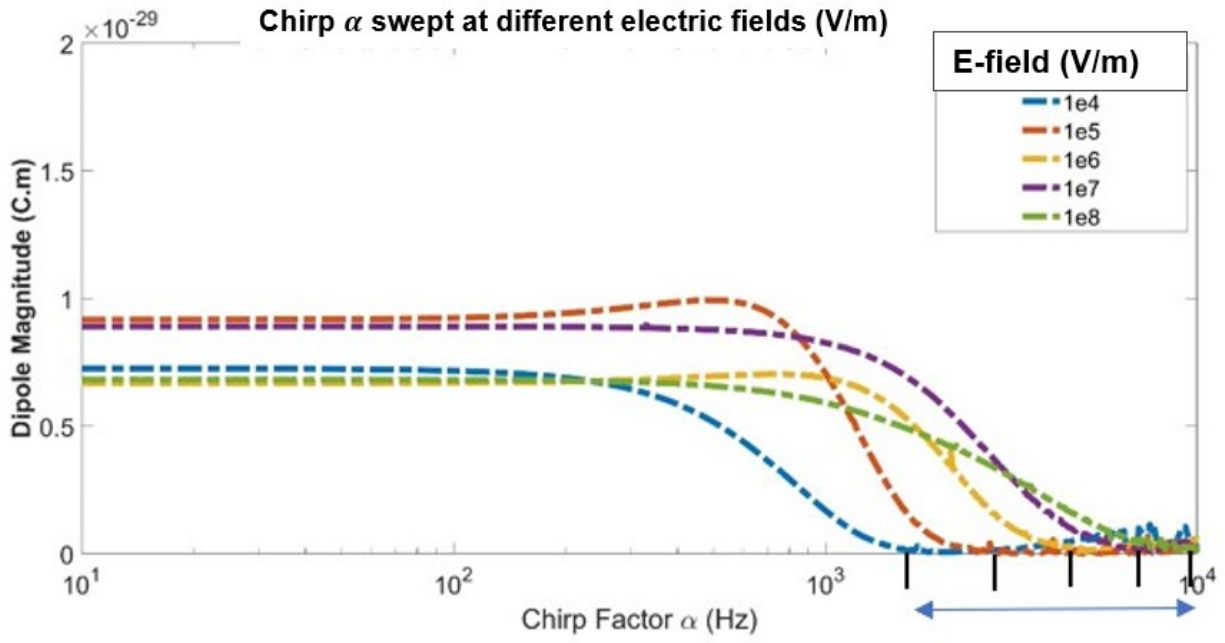

Figure 8: Sweep of chirp from 10 Hz to 10,000 Hz at increasing electric fields. The RMS dipole intensity rolls off and reaches a minimum for each Intensity. That optimal chirp increases with increasing electric field strength.

b. Control with Quadratic Chirp

Another type of chirp used is a non-linear chirp. Here, the quadratic chirp has two Chirp factors α (Hz^2) and β (Hz) described by the equation:

$$E = E_o e^{-i\omega(\alpha t^2+\beta t)t} e^{-\frac{(t-t_0)^2}{(2\tau)^2}},$$

To find an optimal quadratic chirp, a quadratic equation is fitted to the gaussian pulse and initial paramenters are obtained for α and β. The fitting is done as shown below:

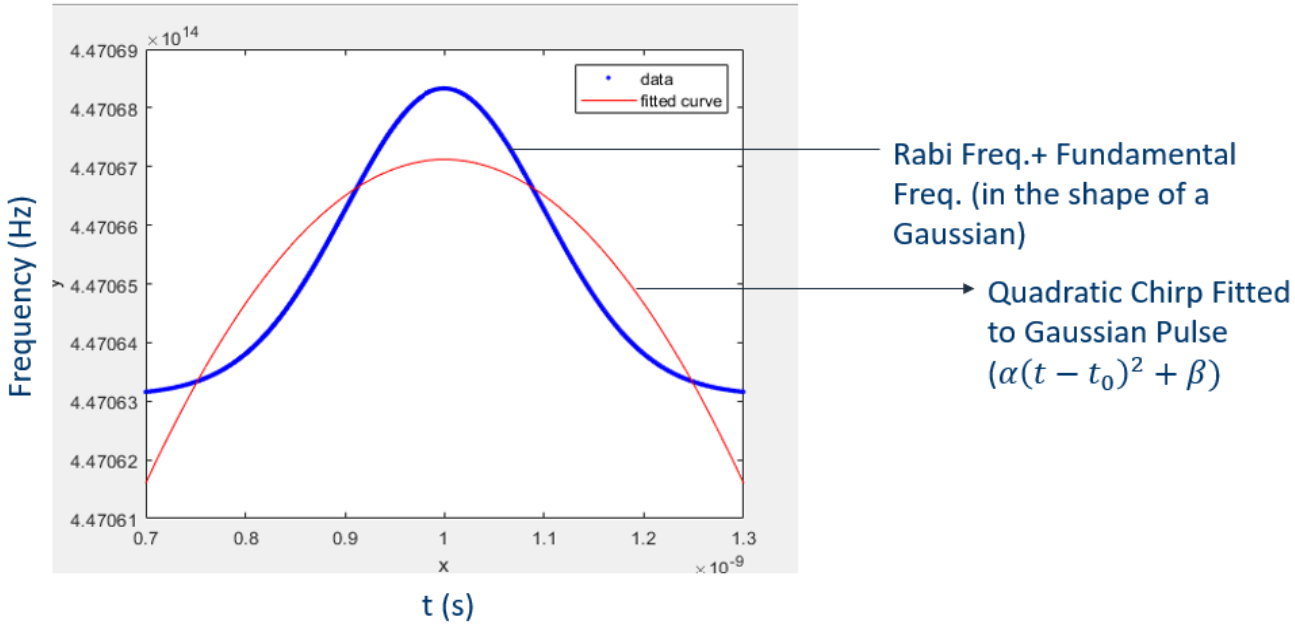

Figure 9: Fitting of the chirp to the Gaussian pulse of e-field 10^5 V/m. The blue is the fundamental frequency plus the Rabi frequency. The red is the quadratic polynomial that fits the Gaussian.

The sum of the fundamental frequency and the rabi frequency is plotted in time. It is a Gaussian. The chirp is fitted to match this using a 2nd degree polynomial fit in MATLAB®. It is fit for a period of the gaussian pulse (from 0.8 to 1.2 ns) to give a good overlap. This

2nd degree polynomial (quadratic) has two parameters α and β which describes the shape of the chirp.

“Confinement” describes the amount with which the dipole moment (being measured) is confined to the energy of the pulse. Mathematically, it is the integral of the square of the dipole moment in a particular range of time (here 0.8 to 1.2 ns, where the majority of the energy of the pulse is contained). The goal of trying to use a quadratic (non-linear) chirp is to try to confine as much of the exciatation to the energy of the pulse

The two parameters are swept together within a small range to find an optimal value in two dimensions. These values would describe the equation of the optimal chirp.

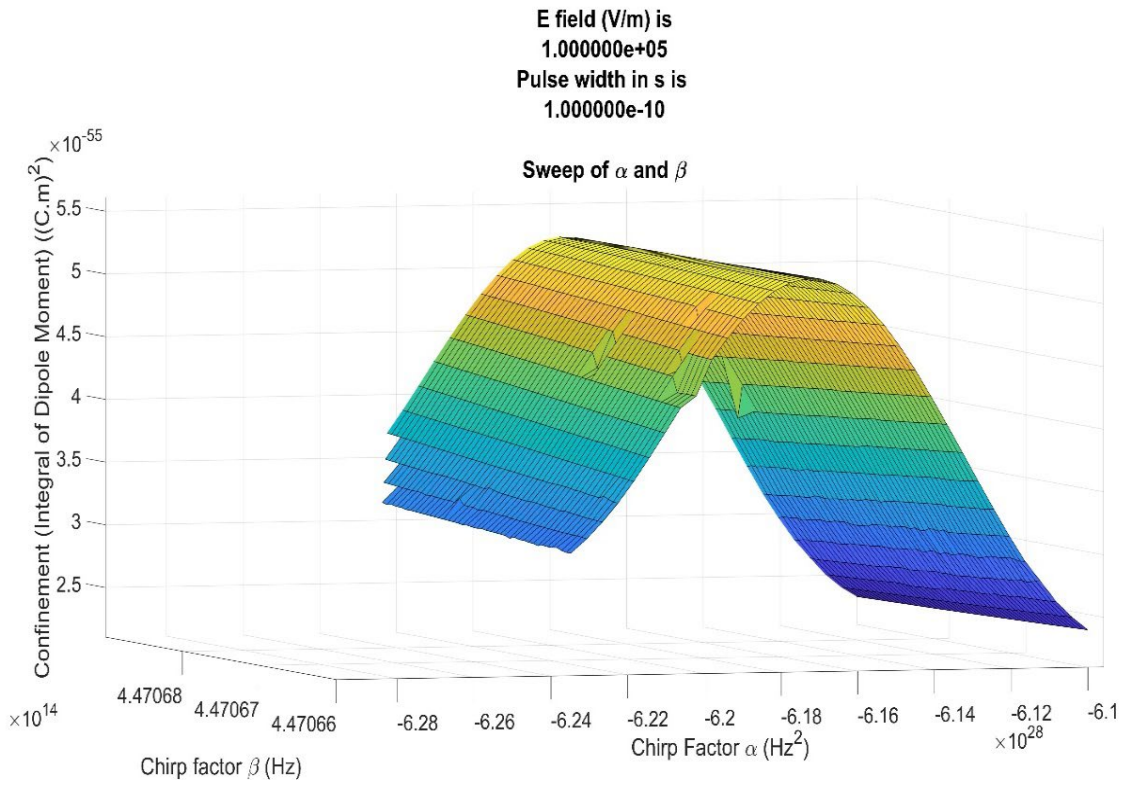

Figure 10 Surface plot varying both chirp parameters in the quadric chirp to find an optimal alpha and beta. The quantity being measured is "Confinement" which is the integral of the square of the dipole moment from 0.8 to 1.2 ns (most energy is contained here).

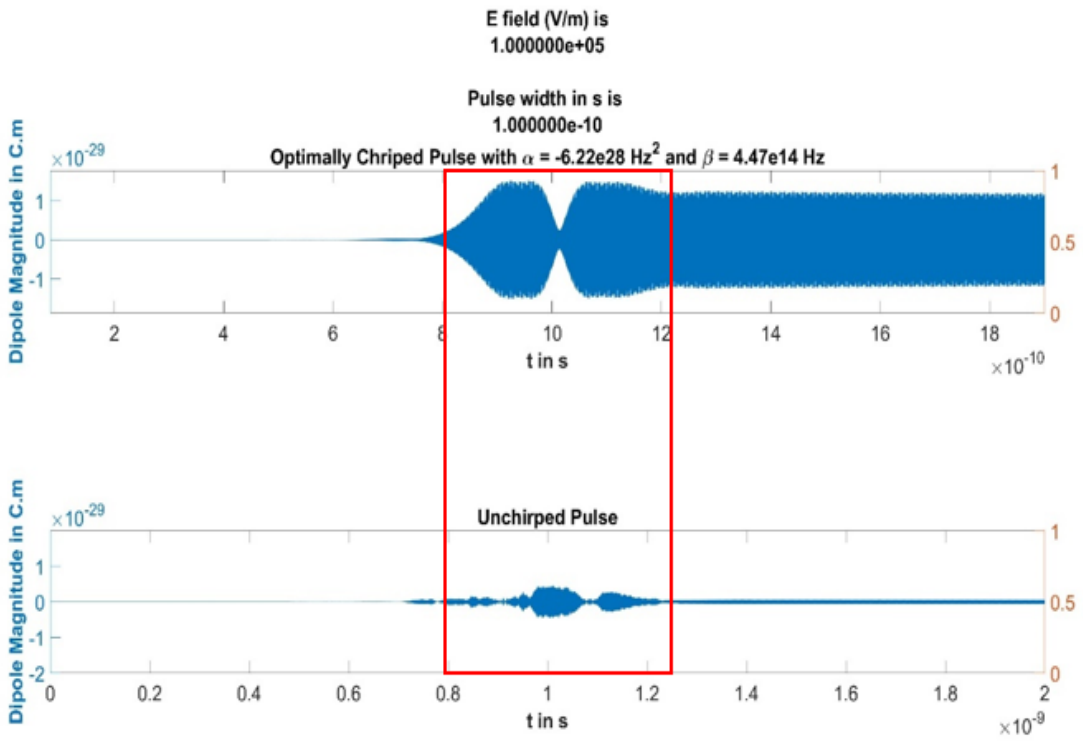

Figure 11 Temporal response to optimal quadratic chirped pulse (above) and unchirped pulse (below). "Confinement" in the range of time (red box) is nearly 10 times in the chirped case.

We see that at with a pulse of this strength (10^5 V/m), the “Confinement” increases almost 10 times with an optimal quadratic chirp compared to the unchirped case.

4. Conclusion

The results in this thesis provide an understanding of the interaction between an electromagnetic field and the optical transition in a diamond NV center (two level quantum system). It also explores the dynamics of population transfer and demonstrates methods for the coherent control of the two-level system with linearly and quadratically chirped gaussian pulses and their effects on the relaxation time in the system and confining the dipole interactions.

These are computational results and would need to be studied practically with diamond NV centers and various factors including temperature, pressure, accuracy of the pulse shapers and broadening effects, among others, should be considered. This system needs laser intensities that are obtained with picosecond and femtosecond lasers but has relaxation times in the nanosecond scale. Other systems with different relaxation times can be studied by adjusting parameters in the code.

Time-resolved spectroscopic methods, such as pump-probe experiments or transient absorption spectroscopy, can provide insights into the dynamics of electronic transitions and the associated transition dipole moments. These techniques involve excitation of the system with a short laser pulse followed by monitoring the time-dependent changes in the system's response.

It's important to note that the measurement of transition dipole moments can be challenging and often requires careful experimental design and analysis. The choice of measurement technique depends on the nature of the system, the available experimental tools, and the desired accuracy and precision of the measurement.

The use of diamond NV center qubits offers a versatile platform for quantum information processing and quantum sensing and this thesis furthers the understanding of their optical interactions.

REFERENCES

1. Boyd, R. (2008). 6. Nonlinear Optics in the Two-Level Approximation. In *Nonlinear optics* (pp. 277–300). Academic Press.
2. Gali, Á. (2019). Ab Initio Theory of the Nitrogen-Vacancy Center in Diamond. *Nanophotonics*, 8, 1907–1943.
3. Collins, A. T., Thomaz, M. F., & Jorge, M. I. B. (1983). Luminescence Decay Time of the 1.945 eV Centre in Type Ib Diamond. *Journal of Physics,* 16, 2177–2181.
4. Tamarat, Ph. et al. (2006). Stark Shift Control of Single Optical Centers in Diamond. *Physical Review Letters*, 97, 083002.
5. Torosov, B. T., Shore, B. W., & Vitanov, N. V. (2021). Coherent Control Techniques for Two-State Quantum Systems: A Comparative Study. *Physical Review A*, 103, 033110.
6. Jo, H., Lee, H.-G., Guérin, S., & Ahn, J. (2017). Robust Two-Level System Control by a Detuned and Chirped Laser Pulse. *Physical Review A,* 96*,* 033403*.*
7. Ibáñez, S., Peralta Conde, A., Guéry-Odelin, D., & Muga, J. G. (2011). Interaction of Strongly Chirped Pulses with Two-Level Atoms. *Physical Review A*, 84, 013428.
8. Ahmadinouri, F., Hosseini, M., & Sarreshtedari, F. (2019). Investigation Of Robust Population Transfer using Quadratically Chirped Laser Interacting with a Two-Level System. *Physica Scripta,* 94, 105404.
9. Vitanov, N. V., Halfmann, T., Shore, B. W., & Bergmann, K. (2001). Laser-Induced Population Transfer by Adiabatic Passage Techniques. *Annual Review of Physical Chemistry*, 52, 763–809.

APPENDIX

The simulations have been created using MATLAB®. The codes can be found on the GitHub repository below. Please refer to the README file before running them:

https://github.com/Neilalohith/Master-Thesis-UCI